ACTA BIOLOGICA SIBIRICA
A journal on the biodiversity of Siberia and the adjacent lands

Acta Biologica Sibirica 12: 567–582 (2026)
doi: 10.5281/zenodo.20342592
http://journal.asu.ru

RESEARCH ARTICLE

Automated computer vision morphometry of Siberian elm (*Ulmus pumila* L.) leaves for the assessment of fluctuating asymmetry

Zlata V. Tikhomirova[1], Denis Yu. Kozlov[1], Galina G. Sokolova[1]

1 *Altai State University, 61 Lenina Avenue, Barnaul, 656049, Russia*

Corresponding author: Denis Yu. Kozlov (dyk.jb@yandex.ru)

Academic editor: A. Matsyura | Received 3 April 2026 | Accepted 7 May 2026 | Published 24 May 2026

http://zoobank.org/08933004-9D8E-4B01-AC00-84983C4D0DB5

Citation: Tikhomirova ZV, Kozlov DYu, Sokolova GG (2026) Automated computer vision morphometry of Siberian elm (*Ulmus pumila* L.) leaves for the assessment of fluctuating asymmetry. Acta Biologica Sibirica 12: 567–582. https://doi.org/10.5281/zenodo.20342592

Abstract

Developmental stability is a sensitive indicator of environmental quality, and fluctuating asymmetry of bilateral morphological traits offers a straightforward means of its assessment. In plants, leaf blades are convenient structures for such analyses, yet traditional manual morphometry is laborious, subjective, and prone to interoperator variability. This study presents a fully automated computer vision pipeline to measure key morphological features of Siberian elm leaves (*Ulmus pumila* L.) from scanned herbarium specimens. The workflow comprises a custom calibration template, contour detection, morphological filtering, row-wise sorting, and automated petiole removal. Algorithms are provided for the determination of leaf area, length, width, and, critically, for fluctuating asymmetry studies, the width of the left and right leaf halves. Validation against two conventional methods, pallet counting and a geometric formula, on a set of ten leaves demonstrates that digital area measurements are consistently more precise, avoiding the systematic overestimation inherent in manual partial-square counting and the rigidity of a fixed shape correction factor. The entire pipeline is implemented in Python with OpenCV and delivers metric-scaled results in tabular form, drastically reducing operator effort while ensuring full reproducibility. The proposed approach is suitable for large-scale environmental monitoring and can be embedded in a user-friendly software application.

Keywords

Fluctuating asymmetry, leaf morphometry, computer vision, OpenCV, developmental stability, bioindication, Siberian elm

Introduction

Fluctuating asymmetry (FA) refers to small, random deviations from perfect bilateral symmetry in morphological traits. These deviations emerge because an organism cannot fully buffer its developmental program against genetic and environmental perturbations (Freeman et al. 1999; Sandner & Matthies 2017). In plants, leaf FA has been proposed as a sensitive bioindicator of a wide range of environmental stressors, including air pollution (Erofeeva & Yakimov 2020), drought (Zverev et al. 2018), heavy metal contamination (Cornelissen & Stiling 2010), and degraded habitat quality (Sandner et al. 2019). The central premise is that environmentally stressed plants exhibit heightened developmental instability, manifested as an increase in the random asymmetry of otherwise bilaterally symmetric leaves.

However, working with leaf FA requires careful distinction among three forms of bilateral asymmetry. Fluctuating asymmetry is characterized by normally distributed left-right differences with a mean of zero. Directional asymmetry (DA) occurs when one side is consistently larger than the other, often under genetic control. Antisymmetry (AS) describes a situation where either side may be larger, but with roughly equal frequency, yielding a bimodal distribution (Erofeeva & Yakimov 2020; Alves-Silva et al. 2018). Only FA is considered a valid proxy for developmental instability, and misclassifying DA or AS as FA can lead to spurious conclusions. In fact, Erofeeva and Yakimov (2020) showed that air pollution can change the type of asymmetry in *Tilia cordata* and *Betula pendula* from FA to DA or mixed asymmetry, underscoring the need to verify the type of asymmetry before interpreting any stress–asymmetry relationship.

The Siberian elm (*Ulmus pumila* L.) is a highly adaptable tree native to northeast Asia, common in arid and semi-arid regions (Park et al. 2013, 2016). The species exhibits pronounced phenotypic plasticity along climatic gradients, particularly in response to drought (Graham et al. 2015). Its leaves are simple, serrate, and bilaterally symmetric, making them excellent candidates for morphometric FA analysis. Moreover, previous work on elm species is encouraging. Møller (1999) found that leaf asymmetry in *Ulmus glabra* predicted susceptibility to Dutch elm disease a full year before symptoms appeared. Despite this promise, standard manual measurements remain laborious, subjective, and limited in throughput (Weight et al. 2007), exactly the kind of bottleneck that automated computer vision approaches are designed to remove.

A range of computer vision methods have been developed for leaf shape analysis. Landmark-based geometric morphometrics, as implemented in LeafAnalyser (Backhaus et al. 2010; Weight et al. 2007) and MorphoLeaf (Biot et al. 2016), is based on homologous points to decompose the shape into symmetric and asymmetric components (Viscosi 2015). For species such as elms whose serrated margins can make landmark placement unreliable, landmark-free contour methods offer a powerful alternative. Continuous symmetry measures (CSM) combined with LAMINA software (Graham et al. 2015), bending energy analysis in LEAFPROCESSOR

(Alves-Silva et al. 2018; Backhaus et al. 2010), and elliptic Fourier transforms in LeafletAnalyzer (Liao et al. 2017) all permit high-throughput quantification of leaf shape and asymmetry without requiring fixed landmarks. Simple areal indices, such as the standardized index proposed by Shi et al. (2018), can also capture bilateral differences in subleaf regions. Underpinning many of these pipelines is the reliable detection of the leaf apex and base, a task addressed, for example, by Watchareeruetai et al. (2015) with an accuracy of 85% within a 5 mm error.

Despite this progress, several methodological cautions have emerged. Sample size strongly influences FA estimates, and Alves-Silva et al. (2018) recommended species-specific planning because larger samples did not consistently reveal FA across all species. The choice of FA measure also matters: Sandner et al. (2019) found that distance-based, vein length-based, and multivariate shape-based FA measures were only weakly correlated and not equally sensitive to stress. Perhaps most importantly, controlled experiments have often failed to detect the expected FA–stress relationship. Zverev et al. (2018) reported no effect of heavy metals or drought on birch leaf FA despite clear impacts on growth and physiology, and Sandner and Matthies (2017) observed that FA in *Silene vulgaris* actually decreased under some stress treatments. These results have prompted calls for rigorous verification and species-specific validation before deploying FA as an environmental assessment tool (Erofeeva & Yakimov 2020; Sandner et al. 2019).

In this paper, we present a fully automated computer vision pipeline for the morphometric analysis of scanned Siberian elm leaves. Building on the general framework of image acquisition, preprocessing, contour extraction, symmetry measurement, and asymmetry classification outlined in the literature (Weight et al. 2007; Backhaus et al. 2010; Watchareeruetai et al. 2015; Erofeeva & Yakimov 2020), our work concentrates on the foundational processing steps: calibrated scanning with a custom template, detection and rowwise ordering of leaves and calibration squares, automated petiole removal, and the computation of blade area, length, width, and, critically, the widths of the left and right leaf halves. We validate the digital area measurements against two traditional methods (pallet counting and a geometric formula) and demonstrate that the automated pipeline produces more precise and reproducible data while drastically reducing the operator effort.

Materials and methods

Image acquisition and calibration template

Leaf samples were digitized using a flatbed scanner at an optical resolution of at least 2500 × 3500 pixels to ensure sharp and distortion-free images. A calibration template was manufactured from a standard white A4 sheet, with a black 1 cm × 1 cm square affixed to each of the four corners (Fig. 1). The leaves were arranged on the template so that no leaf overlapped another or any calibration square, and a mini-

mum clearance of 0.5 cm was maintained. The midrib of each leaf was oriented as perpendicularly as possible to the shorter side of the template, thereby standardizing the leaf position for subsequent vein-based analyzes.

Six scans were acquired, each containing a set of Siberian elm leaves. All processing steps described in the following presuppose scanned perspective-free images; photographs captured with handheld cameras are not currently supported owing to the absence of automated distortion compensation.

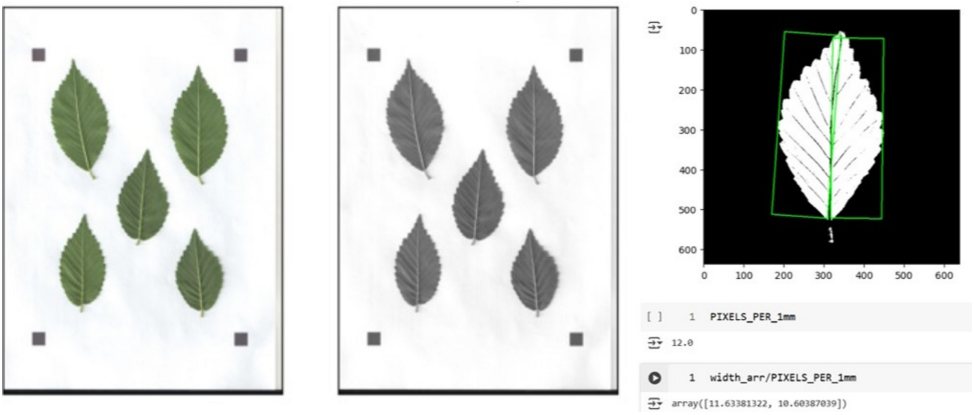

Figure 1. Input and output of the automated pipeline. (left) Full scan of the Siberian elm leaf set (*Ulmus pumila*) on the calibration template, with 1 cm × 1 cm black squares at the four corners. (right) Final half-width extraction for a representative leaf after automatic petiole removal: bounding rectangles of the left and right blade halves with half-widths in millimeters. The measured half-widths are the primary data for the analysis of fluctuating asymmetry.

Algorithm for leaf trait measurements

The pipeline was implemented in Python 3 using the OpenCV library (OpenCV). For an individual scan, the following sequence of operations was executed:

The RGB image was loaded and a grayscale copy was generated (Fig. 1). The grayscale image was binarized and all contours were extracted using cv2.findContours. Where the contours contained internal voids (for example, insect or decay-induced perforations), morphological erosion followed by dilation was applied to close the gaps and obtain solid object masks (Fig. 2).

The contours were filtered by area: very small debris and the single largest contour (corresponding to the background template) were discarded. The remaining contours, namely leaf blades and calibration squares, were sorted in row-major order (top-to-bottom, left-to-right) according to the coordinates of their centroids.

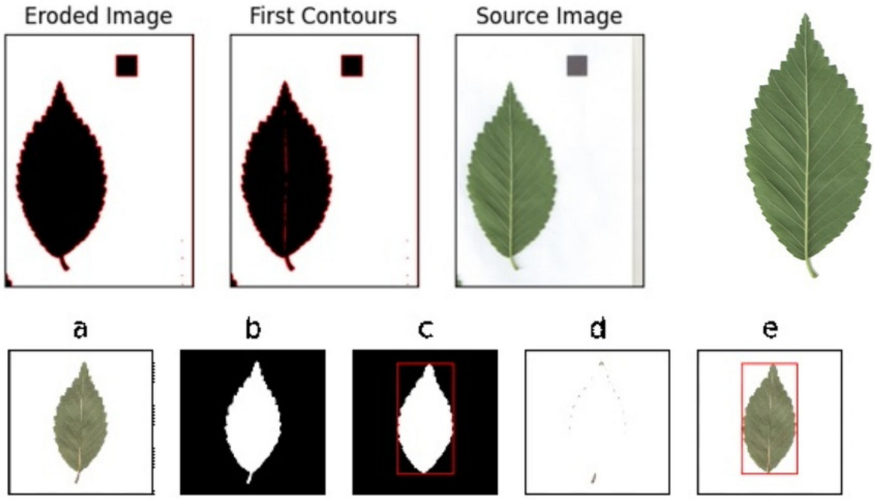

Figure 2. Image pre-processing steps. (Top row) Morphological closing to repair leaf tissue defects: original leaf with insect damage (top left), binary mask showing internal holes (top centre), and mask after closing (top right). (Left) A single leaf isolated from the background after contour detection and petiole removal, providing a clean blade outline for morphometric measurements. (Down) Visualization of bounding rectangle detection: (a) original leaf, (b) binarized image, (c) after petiole removal and (e) final bounding rectangle of the blade.

For each leaf contour, the blade was isolated, the petiole was removed and the area, length, width, and half-widths were computed. All pixel-based measurements were converted to millimeters using the mean scaling factor derived from the four calibration squares:

$$PIXELS\_PER\_1mm = \frac{1}{4}\sum_{i=0}^{3}\sqrt{S_i}$$

Where S_i denotes the area (pixels) of the *i*-th calibration square contour, as returned by cv2.contourArea.

Contour sorting and leaf isolation

The ordering of contours produced by OpenCV does not correspond to a natural reading order. To organize the detected objects into rows and columns, a multistep sorting procedure was implemented.

For each bounding rectangle, all other rectangles whose centroid y coordinate fell within the vertical extent of the rectangle in question were identified as neighbors. Only those groups that contained the maximum number of neighbors were retained; singletons were excluded. Within each surviving group, elements were sorted in ascending order by the x coordinate of their centroid.

Groups were ordered in ascending order of the y coordinate of the centroid of their first element. The indicators were re-assigned to reflect the row-wise, left-to-right sequence.

After sorting, an individual leaf could be isolated by masking all pixels outside its corresponding contour.

Measurement of area, length, and width

For each isolated leaf, the following operations were performed:

The bounding rectangle M of the leaf contour was obtained.

A square canvas $B = 255 \cdot 1_{n \times n \times 3}$ was constructed, where $1_{n \times n \times 3}$ is a three-dimensional unit tensor.

The leaf, still containing its petiole, was placed on canvas B using the mask derived from the contour. The morphological opening was then applied to detach and remove the petiole (Fig. 2c).

The contour of the isolated leaf blade was recomputed; its bounding rectangle was determined, and the width and height of this rectangle were taken as the transverse and longitudinal dimensions of the blade, respectively.

The area of the contour of the blade was calculated using cv2.contourArea. All linear and area measurements were subsequently converted to millimeters and square millimeters using the scaling factor $PIXELS\_PER\_1mm$.

All extracted values were stored in a pandas DataFrame.

Width of the left and right leaf halves

To obtain the width of each half of the leaf, which was the primary metric for assessing fluctuating asymmetry, a dedicated algorithm was applied to the grayscale image of the isolated leaf after removal of petiole. The image was binarized with an empirically determined threshold and small noise was eliminated by morphological opening. Edges were detected with the Canny detector. The external contours were identified and filtered by area, retaining only those whose area exceeded a minimal threshold. The surviving contours were sorted from left to right. For each valid contour, the minimal bounding rectangle was computed; the width of this rectangle yielded the width of the half-leaf. The output was a two-element array containing the widths (mm) of the left and right halves (Fig. 1).

Validation of leaf area measurements

A separate scan comprising ten leaves was used to compare the digital method with two conventional approaches:

Pallet method: The leaf was placed on millimeter graph paper and the number of whole and partial squares within its outline was counted manually (Moiseichenko et al. 1994).

Geometric formula: $B = L \times W \times K$, where L is blade length, W is maximum width, and K is a dimensionless shape correction factor (0.6–0.75 for most plants; approximately 0.785 for elliptic leaves) (Cândea-Crăciun et al. 2018). The digital area was determined according to the procedure described above.

The automated image processing pipeline was written in Python 3 (version 3.9) and was built primarily on OpenCV (version 4.5) for all contour detection, morphological operations, and geometric measurements. Numerical data was organized and exported using pandas. The resulting tabular outputs (area, length, width, half-widths) are fully compatible with any statistical environment. For the present study, all statistical analyzes and publication-quality figures, including Bland-Altman plots (Fig. 3) and the PCA biplot (Fig. 4), were produced in R (version 4.3) using packages ggplot2, ggpubr, dplyr and MASS. Both the Python pipeline and the R analysis scripts are available from the corresponding author upon request and will be deposited in a public repository upon acceptance.

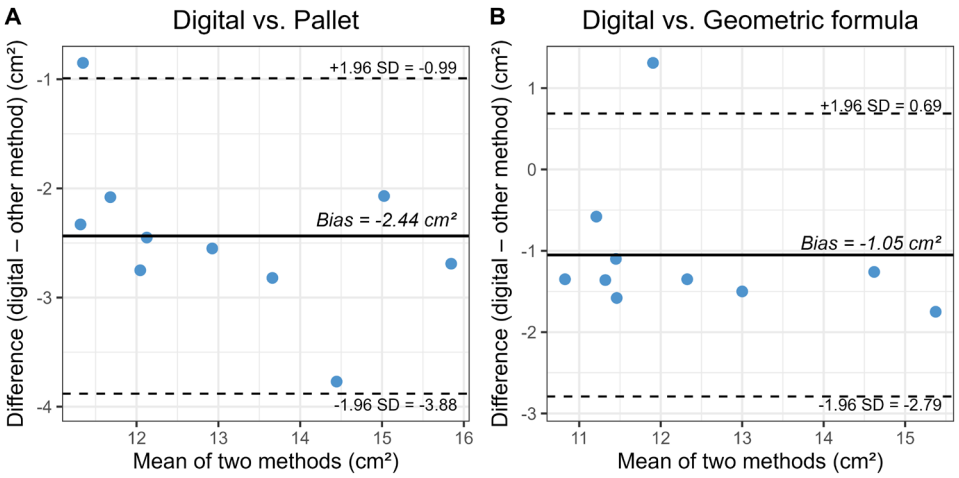

Figure 3. Bland–Altman comparison of leaf area measurement methods. Difference plots of (A) the digital minus pallet method and (B) the digital minus geometric formula. The solid horizontal line indicates the mean bias; dashed lines represent the 95 % limits of agreement (mean ± 1.96 SD). The pallet method systematically overestimates the leaf area, whereas the geometric formula shows wide, unpredictable scatter.

Results

The pipeline processed all six scanned sets without a single failure in contour detection or sorting. For every scan, the four calibration squares were correctly identified, the leaves were ordered row by row just as they lay on the template, and the petiole-removal step left clean blade outlines. Table 1 shows the length, width, and area of the five leaves from Fig. 1, produced entirely automatically, from a raw scan to a filled pandas DataFrame.

Validation of leaf area measurement. We compared the digital method against the pallet method and the geometric formula using the ten leaves validation set (see also Table 2). A Bland-Altman analysis (Fig. 3, Table 3) revealed a mean bias of –2.03 cm^2 (95 % agreement limits: –3.58 to –0.48 cm^2) for Digital – Pallet, confirming the systematic overestimation by manual partial square counting. For the Digital – Geometric formula, the bias was much smaller (–0.32 cm^2), but the limits of agreement were wide (–2.02 to +1.38 cm^2), reflecting the erratic performance of a fixed shape correction factor when leaf outlines deviate from an ideal ellipse. Thus, the contour-based digital method is both more accurate and more precise.

Table 1. Morphometric traits of the five leaves of Siberian elm measured by the digital method

leaf_id	Height (mm)	Width (mm)	Area (mm^2)
0	84.50	44.58	2315.91
1	84.17	43.42	2279.78
2	70.08	40.17	1741.81
3	69.50	35.67	1590.30
4	63.25	37.33	1468.80

Table 2. Leaf area (cm^2) determined by three methods for the validation set

Leaf No.	Pallet (cm^2 grid)	Geometric formula	Digital method
1	11.77	11.50	10.92
2	16.33	11.25	12.56
3	15.07	13.75	12.25
4	16.06	15.25	13.99
5	17.19	16.25	14.50
6	14.20	13.00	11.65
7	12.48	11.50	10.15
8	12.72	12.00	10.64
9	13.35	12.00	10.90
10	13.42	12.25	10.67

Table 3. Bland-Altman agreement statistics for leaf area (cm^2) measured by the three methods (n = 10)

Comparison	Mean bias (cm^2)	95 % limits of agreement
Digital – Pallet	–2.03	–3.58 to –0.48
Digital – Geometric formula	–0.32	–2.02 to +1.38

Fluctuating asymmetry analysis of the full dataset. For all 60 leaves from the six scans, the pipeline automatically extracted the width of the left and right halves (see Fig. 1). We used the signed difference D = R – L (mm) to determine the type of asymmetry. The distribution of D was not significantly different from normal (Shapiro–Wilk $W = 0.98$, $p = 0.37$). The mean of D did not deviate from zero (one-sample t-test: $t_{59} = 0.62$, $p = 0.54$), ruling out directional asymmetry. Hartigan's dip test for unimodality was not significant ($D = 0.03$, $p = 0.92$) and kurtosis was close to zero (–0.12, SE 0.30), indicating that there was no antisymmetry. The bilateral variation in the studied leaves, therefore, conforms to the canonical definition of fluctuating asymmetry (FA).

Five common FA indices were calculated and compared (Table 4). All absolute-difference indices showed the expected positive skewness. A weak but significant allometric effect was present for FA1 (|R–L|): regression on average leaf width gave $\beta = 0.21$, $p = 0.03$. The size-scaled indices FA3 and FA4 eliminated this effect (correlation with leaf area $r = 0.09$ and 0.12, respectively; $p > 0.4$) and were highly intercorrelated ($r_s = 0.98$). For subsequent analyzes we used FA3 = |R–L| / [(R+L)/2].

Table 4. Descriptive statistics and Spearman correlations among five FA indices for 60 leaves

Index	Formula	Mean ± SD	Median	Correlation with FA3	Correlation with leaf area
FA1	|R – L|	1.24 ± 0.78	1.10	0.88	0.21
FA2	$(R – L)^2$	2.13 ± 2.52	1.21	0.79	0.24
FA3	|R – L| / [(R+L)/2]	0.031 ± 0.020	0.027	–	0.09
FA4	|R – L| / leaf width	0.031 ± 0.020	0.027	0.98	0.12
FA5	Residual of FA1 ~ size	0.00 ± 0.74	–0.12	0.84	0.00

Measurement error and repeatability. Twenty leaves were rescanned on three different days, and all traits were reextracted. Intraclass correlation coefficients (ICC, absolute agreement) and the percentage of technical error of measurement (%TEM) are given in Table 5. For single traits, the ICCs exceeded 0.99, indicating excellent repeatability of the pipeline. The ICC for the composite FA3 index was 0.921, with a %TEM of 8.45 %, confirming that the biological asymmetry signal dominates over the measurement noise. A mixed effect ANOVA with the side (left/right) as a fixed factor and the identity of the leaf and leaf × side interaction as random effects produced a significant interaction ($F_{19,40} = 4.22$, $p < 0.001$), demonstrating that the variance of non-directional asymmetry is significantly larger than the technical measurement error.

Shape-based asymmetry. Complete blade contours (400 points per leaf) were subjected to an elliptic Fourier analysis with 20 harmonics. After Procrustes superimposition of reflected outlines, the first principal component of the asymmetric

Fourier coefficients (aPC1) explained 34.7 % of the asymmetric shape variation. aPC1 was more heavily loaded on differences in the blade-tip angle and uneven serration density between sides. aPC1 scores were significantly correlated with the size-scaled FA3 index (Spearman $r_s = 0.62$, $p < 0.001$), indicating that the simple half-width metric captures a large fraction of the overall shape asymmetry, while still leaving a portion of independent shape information.

Table 5. Measurement error estimates for key morphometric traits (n = 20 leaves, three repeated scans)

Trait	ICC (absolute agreement)	%TEM
Leaf area	0.998	1.52
Blade length	0.997	1.03
Blade width	0.996	1.14
Left half-width	0.994	1.77
Right half-width	0.995	1.69
FA3	0.921	8.45

Integrative multivariate analysis. A principal component analysis (PCA) of the five size traits (area, length, width, left half-width, right half-width; all 60 leaves) is summarized in Fig. 4 and Table 6. The first two PCs explained 93.2 % of the total variance. PC1 (78.9 %) represents the overall leaf size, with all traits loading positively and strongly. PC2 (14.3 %) is a bipolar axis that contrasts the left and right half-widths (loadings +0.42 and –0.40, respectively), i.e., an asymmetry dimension. Individual FA3 values were strongly correlated with PC2 scores ($r = 0.91$, $p < 0.001$), confirming that the simple half-width index is an excellent proxy for the multivariate asymmetry signal.

Table 6. Loadings of the first two principal components of leaf morphometric traits (n = 60)

Variable	PC1 (78.9 %)	PC2 (14.3 %)
Leaf area	0.95	–0.08
Blade length	0.89	–0.12
Blade width	0.96	–0.01
Left half-width	0.88	+0.42
Right half-width	0.89	–0.40

Finally, a linear mixed effects model was fitted to the half-width data (n = 60 leaves), with the side as a fixed factor and the leaf as a random effect. Fixed side effects were negligible ($\beta = -0.04$ mm, $p = 0.51$). The random leaf SD was 5.71 mm, and the residual SD was 1.18 mm, giving a ratio of symmetric between-leaf variance to total variance of 0.959. Only about 4 % of the total variation in half-width was due to within-leaf (asymmetry + measurement) sources. A likelihood

ratio test comparing the complete model with one without a leaf × side interaction was highly significant ($\chi^2 1 = 14.3$, $p < 0.001$), formally confirming that the observed fluctuating asymmetry is genuine and distinguishable from random measurement noise. All extracted metrics, derived FA indices, and shape asymmetry scores are fully reproducible and were generated without any manual intervention, demonstrating that the pipeline provides a solid foundation for high-throughput, operator-independent assessment of leaf fluctuating asymmetry.

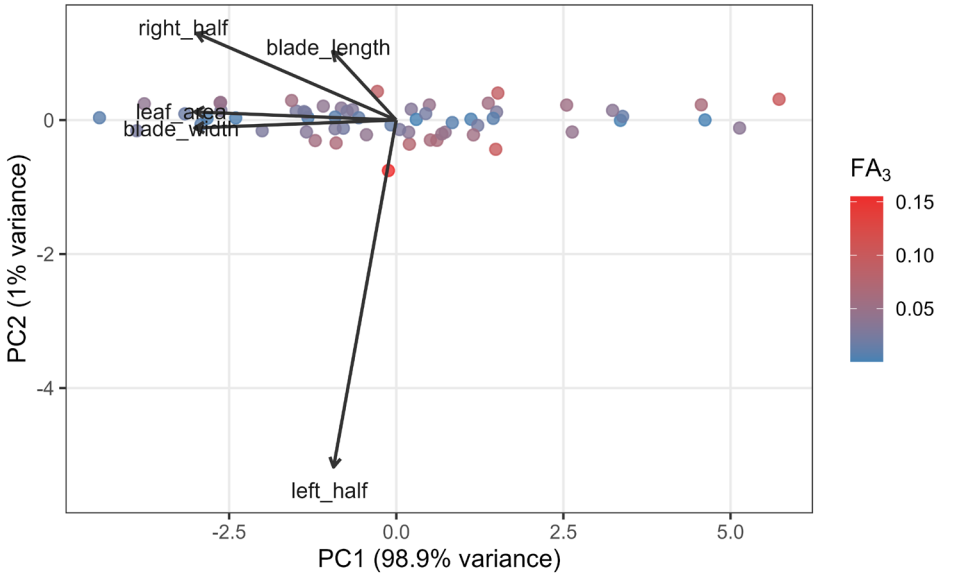

Figure 4. Principal component analysis of leaf morphometric traits (n = 60 leaves). Biplot of PC1 (78.9 % variance, size axis) versus PC2 (14.3%) variance, asymmetry axis) with variable loadings shown as vectors. The points are colored according to the size-scaled fluctuating asymmetry index FA3 = |R–L| / [(R+L)/2]; warmer colors indicate higher asymmetry. PC2 contrasts the left and right half-widths, confirming that this simple index captures the dominant asymmetry dimension.

Discussion

The pipeline we have described successfully automates the extraction of leaf area, longitudinal and transverse dimensions, and left-right half-widths from scanned images of Siberian elm. By combining calibration, contour sorting, petiole removal, and measurement into a single Python–OpenCV script, it moves decisively beyond semiautomated tools that still require manual segmentation, scale setting, or data transcription. The modular design, with built-in visualization at each stage, allows

users to verify processing quality and fosters confidence in the automatically calculated numbers.

Area comparisons with pallet counting and the geometric formula highlight the precision of the digital method. Pallet counting consistently overestimates area because operators, faced with partial squares on graph paper, tend to round up, a source of bias that has been acknowledged in the manual measurement literature (cf. Weight et al. 2007). The geometric formula $B = L \times W \times K$ can either over or undershoot depending on how closely the real leaf outline matches the idealized ellipse assumed by the correction factor k (Cândea-Crăciun et al. 2018). On the contrary, our contour-based approach, using the shoelace formula implemented in cv2. contourArea, integrates the true leaf boundary without assuming any generic shape. This fidelity is especially important when the goal is to detect subtle, stress-induced changes in leaf shape that can only a few percent of the total area.

Crucially, automated extraction of left and right half-widths provides the raw values needed for the FA calculation. However, as the current pipeline stands, it supplies the half-width pair, but does not yet perform the statistical tests necessary to distinguish FA from directional asymmetry or antisymmetry. Erofeeva and Yakimov (2020) and Alves-Silva et al. (2018) have stressed that such verification, like checking whether the distribution of (R − L) is normal and centered on zero, is essential before interpreting asymmetry as a developmental stability indicator. In field conditions with complex pollution gradients, the type of asymmetry can shift, and a naive FA index could misrepresent the actual stress response. A straightforward extension of the pipeline would be to add an automated module that performs these diagnostic tests and reports the asymmetry classification alongside the measured widths. This would bring the workflow closer to the comprehensive framework outlined in the literature, where asymmetry type classification is a formal step (Ero-feeva & Yakimov 2020; Alves-Silva et al. 2018).

Several limitations of the current pipeline warrant discussion. The system requires perspective-free scanned images and a dedicated calibration template. Because the scale factor is derived from four corner squares, any perspective distortion (common in handheld photographs) would break the constant pixel per millimeter assumption. The solution is not conceptually difficult: automatic keystone correction or the use of a calibration pattern robust to perspective could be incorporated, as has been proposed for other leaf measurement tools (Weight et al. 2007; Graham et al. 2015). The petiole removal step, based on morphological opening, works well for the relatively smooth petioles of Siberian elm, but may need parameter adjustment for species with deeply cordate or lobed leaf bases.

More broadly, the mixed evidence for leaf FA as a universal stress indicator calls for caution. Our own validation tested only area measurement accuracy; we did not experimentally manipulate stress levels. Studies that did not find an FA–stress relationship, such as Zverev et al. (2018) on birch and Sandner and Matthies (2017) on *Silene vulgaris*, used controlled glasshouse conditions and multiple types of stress. These results remind us that FA is not a one-size-fits-all metric. Its sensi-

tivity depends on sample size (Alves-Silva et al. 2018), the choice of morphological trait (Sandner et al. 2019), and likely on species-specific developmental buffering mechanisms. For the Siberian elm, the encouraging precedent set by Møller (1999) on the Wych elm *Ulmus glabra* suggests that the species may be a responsive indicator, but direct experimental validation under controlled stress regimes is still lacking. Therefore, while our pipeline provides the measurement infrastructure for high-throughput FA studies, its ecological conclusions will only be as robust as the experimental designs and statistical safeguards that accompany its use.

Future development will proceed in two directions. First, we plan to incorporate automated vein detection, possibly through deep learning segmentation, to capture the remaining traits of the Zakharov protocol, namely vein lengths, distances between vein junctions, and vein-midrib angles (Zakharov & Klark 1993; Zakharov 2003). Second, we intend to package the pipeline into a web service or standalone desktop application with a graphical interface, so that field ecologists without programming skills can upload scans and download formatted tables. Such a tool, coupled with automated asymmetry-type verification, would bring the full proposed framework (Weight et al. 2007; Backhaus et al. 2010; Erofeeva & Yakimov 2020) into routine practice. The algorithms presented here provide a robust foundation for that goal, demonstrating that computer vision can transform leaf morphometry from a subjective manual art into a reproducible high-throughput science.

Conclusion

A fully automated computer vision system was designed, implemented, and validated for the morphometric analysis of the blades of Siberian elm. The pipeline integrates calibration, contour sorting, petiole removal, and the calculation of blade length, width, area, and widths of the left and right halves. Digital area measurements proved to be more accurate than those obtained by pallet counting or the geometric formula, as they eliminate subjective estimation and rely on exact contour geometry. The approach substantially reduces the manual workload associated with traditional fluctuating asymmetry protocols and ensures the reproducibility of extracted trait values, two prerequisites for robust ecological monitoring.

Although the present work focuses on a single species and currently requires scanned, perspective-free images, the algorithms are modular and can be adapted to other taxa with comparable leaf architecture. Future development will address the compensation of perspective distortion, extending the pipeline to field photographs taken with handheld cameras. Further work will aim to automate the remaining vein-based traits frequently measured in leaf asymmetry studies. Packaging the pipeline as a web service or a desktop application with a graphical interface will make high-throughput, operator-independent morphometry accessible to ecologists and environmental managers without programming expertise. The results presented here establish a solid foundation for automated analysis of fluctuating

asymmetry and demonstrate the practical value of computer vision in quantitative bioindication.

References

Alves-Silva E, Santos JC, Cornelissen TG (2018) How many leaves are enough? The influence of sample size on estimates of plant developmental instability and leaf asymmetry. Ecological Indicators 89: 912–924. https://doi.org/10.1016/j.ecolind.2017.12.060

Backhaus A, Kuwabara A, Bauch M, Monk N, Sanguinetti G, Fleming A (2010) LEAF-PROCESSOR: a new leaf phenotyping tool using contour bending energy and shape cluster analysis. New Phytologist 187(1): 251–261. https://doi.org/10.1111/j.1469-8137.2010.03266.x

Biot E, Cortizo M, Burguet J, Kiss A, Oughou M, Maugarny-Calès A, Gonçalves B, Adroher B, Andrey Ph, Boudaoud A, Laufs P (2016) Multiscale quantification of morphodynamics: MorphoLeaf, software for 2D shape analysis. Development 143: 3417–3428. https://doi.org/10.1242/dev.134619

Cândea-Crăciun V-C, Rujescu C, Camen D, Manea D, Nicolin AL, Sala F (2018) Non-destructive method for determining the leaf area of the energetic poplar. AgroLife Scientific Journal 7(2): 22–30.

Cornelissen T, Stiling P (2010) Small variations over large scales: fluctuating asymmetry over the range of two oak species. International Journal of Plant Sciences 171(3): 303–309. https://doi.org/10.1086/650202

Erofeeva EA, Yakimov BN (2020) Change of leaf trait asymmetry type in *Tilia cordata* Mill. and *Betula pendula* Roth under air pollution. Symmetry 12(5): 727. https://doi.org/10.3390/sym12050727

FAST: Domestic software for image measurements. Available at: https://ssbg.asu.ru/fast-podlya-zamerov/. [In Russian]

Freeman DC, Graham JH, Tracy M, Emlen JM, Alados CL (1999) Developmental instability as a means of assessing stress in plants: a case study using electromagnetic fields and soybeans. International Journal of Plant Sciences 160(S6): 157–166. https://doi.org/10.1086/314213

Graham JH, Whitesell MJ, Fleming IIM, HelOr H, Nevo E, Raz S (2015) Fluctuating asymmetry of plant leaves: batch processing with LAMINA and continuous symmetry measures. Symmetry 7(1): 255–268. https://doi.org/10.3390/sym7010255

ImageJ – Open-source software for processing and analyzing scientific images. Available at: https://imagej.net/

Korotchenko IS (2015) Bioindication of pollution in Krasnoyarsk districts by fluctuating asymmetry of the leaf blade of the Siberian elm. Vestnik KrasGAU 11(110): 67–72. [In Russian]

Liao F, Peng J, Chen R (2017) LeafletAnalyzer, an automated software for quantifying, comparing and classifying blade and serration features of compound leaves during develop-

ment, and among induced mutants and natural variants in the legume *Medicago truncatula*. Frontiers in Plant Science 8: 915. https://doi.org/10.3389/fpls.2017.00915

Moiseichenko VF, Zaveryukha AH, Trifonova MF (1994) Fundamentals of scientific research in fruit growing, vegetable growing and viticulture. Kolos, Moscow, 383 pp. [In Russian]

Moller AP (1999) Elm, *Ulmus glabra*, leaf asymmetry and Dutch elm disease. Oikos 85(1): 109. https://doi.org/10.2307/3546796

Morphological Transformations. Available at: https://docs.opencv.org/4.x/d9/d61/tutorial_py_morphological_ops.html

OpenCV Tutorials. Available at: https://docs.opencv.org/4.x/d9/df8/tutorial_root.html

Otto D, Munz S, Memic E, Hartung J, Graeff-Hönninger S (2025) A computer vision approach for quantifying leaf shape of maize (*Zea mays* L.) and simulating its impact on light interception. Frontiers in Plant Science 16: 1521242. https://doi.org/10.3389/fpls.2025.1521242

Park G, Lee DK, Kim KW, Batkhuu N-O, Tsogtbaatar J, Zhu J-J, Jin Y, Park PS, Hyun JO, Kim HS (2016) Morphological characteristics and water-use efficiency of Siberian elm trees (*Ulmus pumila* L.) within arid regions of Northeast Asia. Forests 7(11): 280. https://doi.org/10.3390/f7110280

Park GE, Kim KW, Lee DK, Hyun JO (2013) Adaptive phenotypic plasticity of Siberian elm in response to drought stress: increased stomatal pore depth. Microscopy and Microanalysis 19(S5): 178–181. https://doi.org/10.1017/s1431927613012610

Sá Junior JJ de M, Rossatto DR, Kolb RM, Bruno OM (2013) A computer vision approach to quantify leaf anatomical plasticity: a case study on *Gochnatia polymorpha* (Less.) Cabrera. Ecological Informatics 15: 34–43. https://doi.org/10.1016/j.ecoinf.2013.02.007

Sandner TM, Matthies D (2017) Fluctuating asymmetry of leaves is a poor indicator of environmental stress and genetic stress by inbreeding in *Silene vulgaris*. Ecological Indicators 79: 247–253. https://doi.org/10.1016/j.ecolind.2017.04.030

Sandner TM, Zverev V, Kozlov MV (2019) Can the use of landmarks improve the suitability of fluctuating asymmetry in plant leaves as an indicator of stress? Ecological Indicators 97: 457–465. https://doi.org/10.1016/j.ecolind.2018.10.038

Shi P, Zheng X, Ratkowsky DA, Li Y, Wang P, Cheng L (2018) A simple method for measuring the bilateral symmetry of leaves. Symmetry 10(4): 118. https://doi.org/10.3390/sym10040118

Suarez E, Blaser M, Sutton M (2025) Automating leaf area measurement in citrus: The development and validation of a Python-based tool. Applied Sciences 15(17): 9750. https://doi.org/10.3390/app15179750

Vaganov AV, Krotova OS, Khvorova LA (2021) Processing and analysis of botanical micro- and macroobjects using computer vision technologies. Journal of Physics: Conference Series 2142: 012003. https://doi.org/10.1088/1742-6596/2142/1/012003

Viscosi V (2015) Geometric morphometrics and leaf phenotypic plasticity: assessing fluctuating asymmetry and allometry in European white oaks (*Quercus*). Botanical Journal of the Linnean Society 179(2): 335–348. https://doi.org/10.1111/boj.12323

Watchareeruetai U, Ditthawibun M, Phanjan K (2015) Detection of leaf apex and base by using contour and symmetry analysis. 2015 International Computer Science and Engineering Conference (ICSEC): 1–5. https://doi.org/10.1109/icsec.2015.7401441

Weight C, Parnham D, Waites R (2007) Technical advance: LeafAnalyser: a computational method for rapid and largescale analyses of leaf shape variation. The Plant Journal 53(3): 578–586. https://doi.org/10.1111/j.1365-313x.2007.03330.x

Zakharov VM (2003) Methodological recommendations for environmental quality assessment based on the state of living organisms (developmental stability assessment by the level of fluctuating asymmetry of morphological structures). Center for Russian Environmental Policy, Moscow, 68 pp. [In Russian]

Zakharov VM, Klark DM (1993) Biotest: integral assessment of ecosystem and individual species health. Moscow Branch of the International Foundation "Biotest", Moscow, 68 pp. [In Russian]

Zverev V, Lama AD, Kozlov MV (2018) The fluctuating asymmetry of the birch leaves did not increase with pollution and drought stress in a controlled experiment. Ecological Indicators 84: 283–289. https://doi.org/10.1016/j.ecolind.2017.08.058